Korean J. Math. **31** (2023), No. 4, pp. 419–431
https://dx.doi.org/10.11568/kjm.2023.31.4.419

A NON-OVERLAPPING DOMAIN DECOMPOSITION METHOD FOR A DISCONTINUOUS GALERKIN METHOD: A NUMERICAL STUDY

Eun-Hee Park

Abstract. In this paper, we propose an iterative method for a symmetric interior penalty Galerkin method for heterogeneous elliptic problems. The iterative method consists mainly of two parts based on a non-overlapping domain decomposition approach. One is an intermediate preconditioner constructed by understanding the properties of the discontinuous finite element functions and the other is a preconditioning related to the dual-primal finite element tearing and interconnecting (FETI-DP) methodology. Numerical results for the proposed method are presented, which demonstrate the performance of the iterative method in terms of various parameters associated with the elliptic model problem, the finite element discretization, and non-overlapping subdomain decomposition.

1. Introduction

Let Ω be a bounded polygonal domain in $\mathbb{R}^2$ and $f \in L_2(\Omega)$. We consider the following model problem: Find $u \in H_0^1(\Omega)$ such that

$$\int_\Omega \rho \nabla u \cdot \nabla v \, dx = \int_\Omega f v \, dx \qquad \forall\, v \in H_0^1(\Omega), \tag{1}$$

where ρ may vary inside the domain Ω. The model problem (1) can be discretized by symmetric interior penalty (SIPG) methods [3, 5, 10, 22, 25]. The SIPG method is one of the best known discontinuous Galerkin (DG) methods; cf. [2, 23] and the references therein. In this paper we will propose an iterative method for the SIPG method based on a non-overlapping domain decomposition (DD) approach.

There have been various studies on non-overlapping DD methods for discontinuous finite element methods; cf. [1, 4, 5, 8, 9, 11, 12, 15–17]. The most advanced iterative algorithms based on non-overlapping DD are represented by the balancing domain decomposition by constraints (BDDC) and the FETI-DP methodologies; cf. [7, 13, 14, 18–21].

Received September 3, 2023. Revised October 18, 2023. Accepted October 19, 2023.
2010 Mathematics Subject Classification: 65F10, 65N30, 65N55.
Key words and phrases: non-overlapping domain decomposition, discontinuous Galerkin, preconditioner, FETI-DP.
The work was supported by the National Research Foundation of Korea grant funded by Ministry of Science and ICT (NRF-2019R1F1A1060746).

Among the papers referenced above, the works in [5, 12] are the most relevant to the study in this paper. Below, we will briefly describe the key features of the method proposed in this paper compared to those previous works.

Differently from continuous finite element methods, DG methods have the bilinear forms, which include the term that penalizes the jumps of discontinuous finite element functions across the element boundaries. This difference makes it difficult to develop non-overlapping DD methods for DG methods.

The work in [5] proposes a BDDC algorithm for the same problem treated in this paper, which overcomes the difficulty of the DG coupling across the interface by introducing a subspace decomposition of the discontinuous finite element space. On the other hand, the work in [12] proposes a FETI-DP algorithm for a DG method. The difficulty is overcome by introducing the enlarged subdomain problems that include extra unknowns associated with neighboring subdomains. As a result, the size of the subdomain problems associated with the subdomain interface is doubled compared to the similar algorithms developed for continuous finite element methods. Considering those properties of two methods discussed above, in this paper, we develop an iterative method based on the FETI-DP methodology by applying a variant of a subspace decomposition introduced in [5].

The rest of the paper is organized as follows. In Section 2 we introduce the discrete problem resulting from the SIPG method. We then propose an iterative method for solving the discrete problem based on a non-overlapping DD approach in Section 3. In Section 4, we present the numerical study for the proposed methods. Finally, the conclusion is stated in Section 5.

To avoid the proliferation of constants, throughout the paper we will use $A \lesssim B$ and $A \gtrsim B$ to represent the statements that $A \leq (\text{constant})B$ and $A \geq (\text{constant})B$, where the positive constant is independent of the mesh size, the subdomain size, the number of subdomains, and the constant ρ. The statement $A \approx B$ is equivalent to $A \lesssim B$ and $A \gtrsim B$.

2. A discontinuous Galerkin discrete problem

Let $\Omega_1, \cdots, \Omega_J$ be polygonal subdomains of Ω that form a non-overlapping decomposition of Ω. We assume that the diffusion coefficient ρ equals a positive constant ρ_j on the subdomain Ω_j for $1 \leq j \leq J$; cf. Figure 4 and Figure 5.

Let $\mathcal{T}_h$ be a simplicial triangulation of Ω aligned with $\Omega_1, \cdots, \Omega_J$ and

$$X_h = \{v \in L_2(\Omega) : v|_T \in P_1(T) \quad \forall T \in \mathcal{T}_h\} \tag{2}$$

be the discontinuous P_1 finite element space associated with $\mathcal{T}_h$; cf. Figure 2(a) and Figure 2(b). The model problem (1) is discretized by the following SIPG method [3, 5, 10, 22, 25]: Find $u_h \in X_h$ such that

$$a_h(u_h, v) = \int_\Omega f v \, dx \qquad v \in X_h, \tag{3}$$

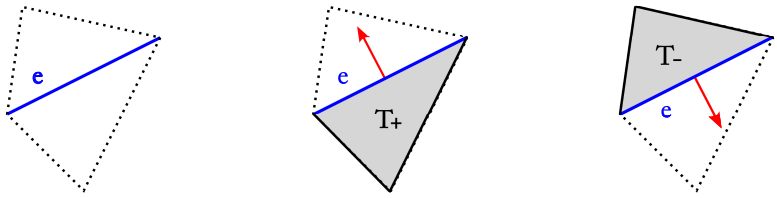

FIGURE 1. Left figure: an edge e shared by two triangles; Center figure: T_+ and $\mathbf{n}_+$; Right figure: T_- and $\mathbf{n}_-$.

where

$$a_h(v,w) = \sum_{T\in\mathcal{T}_h}\int_T \rho\nabla v\cdot\nabla w\,dx + \eta\sum_{e\in\mathcal{E}_h}\frac{\rho_e}{|e|}\int_e [\![v]\!]\cdot[\![w]\!]\,ds - \sum_{e\in\mathcal{E}_h}\int_e \left(\{\!\{\rho\nabla v\}\!\}\cdot[\![w]\!] + \{\!\{\rho\nabla w\}\!\}\cdot[\![v]\!]\right)ds. \tag{4}$$

Here η is a positive penalty parameter, $\mathcal{E}_h$ is the set of the edges of $\mathcal{T}_h$ and $|e|$ is the length of the edge e. Depending on whether an edge e is interior to Ω or along $\partial\Omega$, the weight ρ_e, the jump $[\![v]\!]$, the average $\{\!\{\rho\nabla v\}\!\}$ for vector functions and the average $\{\!\{v\}\!\}$ for scalar functions are defined differently as described in Table 1. For an edge e interior to Ω, two triangles that share the edge e are denoted by T_+ and T_-, where the unit outer normals along $\partial T_\pm$ on the edge e are in opposite directions; cf. Figure 1. For the triangles $T_\pm$, we use the following notations:

$$\rho_\pm = \rho\big|_{T_\pm},\quad v_\pm = v|_{T_\pm},\quad \beta_+ = \frac{\rho_+}{\rho_- + \rho_+},\quad \beta_- = \frac{\rho_-}{\rho_- + \rho_+}.$$

TABLE 1. Definitions of the average operator for scalar functions and the notations that appear in the SIPG bilinear form $a_h(\cdot,\cdot)$, where $\mathbf{n}_\pm$ are the unit outer normals along $\partial T_\pm$ and $\mathbf{n}$ is the unit normal pointing towards the outside of Ω.

	ρ_e	$[\![v]\!]$	$\{\!\{\rho\nabla v\}\!\}$	$\{\!\{v\}\!\}$
e shared by $T_\pm$	$\frac{2\rho_-\rho_+}{\rho_-+\rho_+}$	$v_+\mathbf{n}_+ + v_-\mathbf{n}_-$	$\beta_+(\rho_-\nabla v_-) + \beta_-(\rho_+\nabla v_+)$	$\beta_- v_- + \beta_+ v_+$
e along $\partial\Omega$	ρ	$v\mathbf{n}$	$\rho\nabla v$	$-$

To develop an efficient iterative solver for the problem (3), we consider the following equivalent algebraic form:

$$\boldsymbol{A}\boldsymbol{u} = \boldsymbol{f}, \tag{5}$$

where $\boldsymbol{A}$ is the stiffness matrix, $\boldsymbol{u}$ is the unknowns vector associated with the degrees of freedom of X_h, and $\boldsymbol{f}$ is the vector corresponding to the right-hand side of (3).

REMARK 2.1. Let $\mathcal{V}_h$ be the set of vertices of the triangles in $\mathcal{T}_h$ defined by

$$\mathcal{V}_h = \{(p,T) : p \text{ is a vertex of the triangle } T \text{ in } \mathcal{T}_h\}.$$

We use the values of the discontinuous P_1 finite element functions at the vertices in $\mathcal{V}_h$ as the degrees of freedom. Accordingly, the function v in X_h has one degree of freedom (dof) associated with each vertex in $\mathcal{V}_h$, which is represented by '$\circ$' in Figure 2(b).

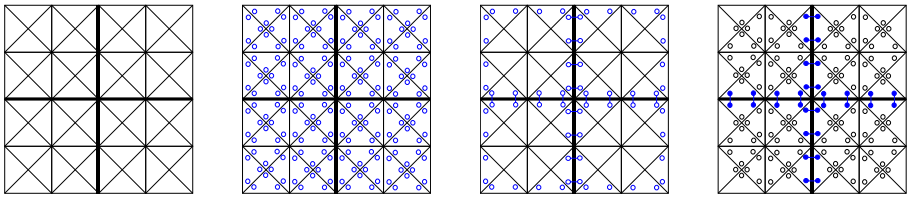

(a) (b) (c) (d)

FIGURE 2. (a) A triangulation $\mathcal{T}_h$ and a non-overlapping domain partition of Ω with the interface Γ in thick lines. (b) Degrees of freedom of X_h. (c) Degrees of freedom of $X_{h,D}$. (d) Degrees of freedom of $X_{h,C}$.

REMARK 2.2. Based on the coercivity property of $a_h(\cdot,\cdot)$ for a sufficiently large penalty parameter η, we have that the stiffness matrix $\boldsymbol{A}$ is symmetric positive-definite (SPD); cf. [5, 23]. In addition, the following estimate holds:

$$\kappa(\boldsymbol{A}) = \frac{\lambda_{\max}(\boldsymbol{A})}{\lambda_{\min}(\boldsymbol{A})} \lesssim \frac{\rho_{\max}}{\rho_{\min}} h^{-2}, \tag{6}$$

where $\rho_{\max} = \max_{x\in\Omega} \rho(x)$, $\quad \rho_{\min} = \min_{x\in\Omega} \rho(x)$.

3. A non-overlapping DD method

In this section we suggest an iterative method for solving the linear system (5). The iterative method consists mainly of two parts based on a non-overlapping DD approach. One is an intermediate preconditioner constructed by understanding the properties of the discontinuous finite element functions. The other is a preconditioning algorithm related to the FETI-DP methodology.

3.1. An intermediate preconditioner.

Let $\Gamma = \left(\bigcup_{j=1}^{J} \partial\Omega_j\right) \setminus \partial\Omega$ be the interface of the subdomains; cf. Figure 2(a). Note that the discontinuous P_1 finite element space X_h is decomposed into two subspaces as follows:

$$X_h = X_{h,D} \oplus X_{h,C}, \tag{7}$$

where

$$X_{h,D} = \{v \in X_h : \{\!\{v\}\!\} = 0 \text{ on the edges on } \Gamma \text{ and } v \text{ vanishes at the vertices in } \mathcal{V}_I\}$$

and

$$X_{h,C} = \left\{ v \in X_h : [\![v]\!] = 0 \text{ on the edges in } \mathcal{E}_h \text{ that are subsets of } \bigcup_{j=1}^{J} \partial\Omega_j \right\}.$$

The set $\mathcal{V}_I$ of interior vertices (cf. black $\circ$ in Figure 2(d)) is defined by

$$\mathcal{V}_I = \left\{ (p,T) \in \mathcal{V}_h : \text{ both edges that share } p \text{ are disjoint from } \bigcup_{j=1}^{J} \partial\Omega_j \right\}.$$

REMARK 3.3. The decomposition in (7) was considered as part of the subspace decomposition introduced in [5]. The work in [5] proposes a BDDC preconditioner based on the subspace decomposition as follows:

$$X_h = X_{h,D} \oplus C_1 \oplus C_2,$$

where C_1 and C_2 are the orthogonal subspaces of $X_{h,C}$ associated with $a_h(\cdot,\cdot)$.

REMARK 3.4. The degrees of freedom of the functions in $X_{h,C}$ and $X_{h,D}$ are described in Figure 2(c) and Figure 2(d), respectively. The function in $X_{h,D}$ has one dof represented by '$\circ$—$\circ$', which is related to a pair of neighboring vertices on Γ, and one dof represented by '$\circ$', which corresponds to each vertex on $\partial\Omega$. On the other hand, the function in $X_{h,C}$ has one dof represented by '$\bullet$—$\bullet$', which is related to a pair of neighboring vertices on Γ, and one dof represented by '$\circ$', which corresponds to each vertex in $\mathcal{V}_I$.

REMARK 3.5. The localization of the bilinear form $a_h(\cdot,\cdot)$ plays an important role in developing efficient iterative solvers for (5); cf. Remark 3.7. From this point of view, the subdomain decomposition (7) was proposed in the author's work [5].

By understanding the properties of the functions in X_h based on (7), we can construct a preconditioner $\boldsymbol{P}_1$ for $\boldsymbol{A}$ defined by

$$\boldsymbol{P}_1 = \boldsymbol{I}_D \boldsymbol{A}_D^{-1} \boldsymbol{I}_D^t + \boldsymbol{I}_C \boldsymbol{A}_C^{-1} \boldsymbol{I}_C^t. \tag{8}$$

Here $\boldsymbol{A}_D$ and $\boldsymbol{A}_C$ are the matrix representation of the SPD operators

$$A_{h,D} : X_{h,D} \longrightarrow X_{h,D}^{'} \quad \text{and} \quad A_{h,C} : X_{h,C} \longrightarrow X_{h,C}^{'}$$

defined by

$$\langle A_{h,D} v, w\rangle = a_h(v,w) \qquad \forall\, v, w \in X_{h,D}, \tag{9}$$

$$\langle A_{h,C} v, w\rangle = a_h(v,w) \qquad \forall\, v, w \in X_{h,C}, \tag{10}$$

and the matrices $\boldsymbol{I}_D$ and $\boldsymbol{I}_C$ correspond to the natural injections

$$I_{h,D} : X_{h,D} \longrightarrow X_h \quad \text{and} \quad I_{h,C} : X_{h,C} \longrightarrow X_h. \tag{11}$$

From (7), (9) and (10), it is noted that the following property holds that for any $v \in X_h$,

$$a_h(v,v) \approx \langle A_{h,D} v_D, v_D\rangle + \langle A_{h,C} v_C, v_C\rangle, \tag{12}$$

where $v = I_{h,D} v_D + I_{h,C} v_C$ is the unique decomposition with respect to the spaces $X_{h,D}$ and $X_{h,C}$; cf. Lemma 2.7 in [5]. Therefore by the theory of additive Schwarz preconditioner [6, 24], we have

$$\kappa(\boldsymbol{P}_1 \boldsymbol{A}) = \frac{\lambda_{\max}(\boldsymbol{P}_1 \boldsymbol{A})}{\lambda_{\min}(\boldsymbol{P}_1 \boldsymbol{A})} \approx 1. \tag{13}$$

REMARK 3.6. Based on (13), the iterative solver accompanied by the preconditioner $\boldsymbol{P}_1$ is theoretically optimal since the condition number estimate is independent of the mesh size h, that is, the problem size.

In addition to the optimality in Remark 3.6, we should look at the practical efficiency of the iterative solver. The solver $\boldsymbol{A}_D^{-1}$ in $\boldsymbol{P}_1$ can be implemented efficiently because the system involving $\boldsymbol{A}_D$ is reduced to a relatively small system related to the degrees of freedom at corner vertices; cf. Figure 2(c). On the other hand, the

solver $\boldsymbol{A}_C^{-1}$ in $\boldsymbol{P}_1$ is the global solver because of the properties of the functions in $X_{h,C}$; cf. Figure 2(d). Therefore, we need to replace the solver $\boldsymbol{A}_C^{-1}$ by a better preconditioner in order to develop efficient iterative solvers in practice.

3.2. An iterative method based on non-overlapping DD.

In order to design an efficient solver for replacing the global solver $\boldsymbol{A}_C^{-1}$, we consider the following problem involving $\boldsymbol{A}_C^{-1}$:

Given $g \in X'_{h,C}$, find $w \in X_{h,C}$ such that

$$\langle A_{h,C} w, v\rangle = \langle g, v\rangle \qquad \forall\, v \in X_{h,C}, \tag{14}$$

where $\langle g, v\rangle = \int_\Omega gv\, dx$.

The FETI-DP method is one of the most advanced non-overlapping DD algorithms, which is based on the Lagrangian method; cf. [7, 13, 14, 19, 21] and the references therein. The method enforces weakly the continuity constraint across the interface except for corner vertices by introducing Lagrange multipliers, while the constraint at corner vertices is imposed in a strong manner.

To weaken the properties of the globally coupled $\boldsymbol{A}_C$, we next introduce the subspace $\hat{X}_h$ of X_h defined by

$$\begin{aligned}\hat{X}_h = \{v \in X_h : v &\text{ is continuous at the corner vertices across } \Gamma \\ &\text{and vanishes on } \partial\Omega\}\,;\end{aligned} \tag{15}$$

cf. Figure 3(a).

Noting that $X_{h,C}$ is a subspace of $\hat{X}_h$, we can define a projection $P_\Gamma : \hat{X}_h \longrightarrow X_{h,C}$ by the average operator presented in Table 1:

$$P_\Gamma v = \{\!\{v\}\!\} \text{ on an edge on } \Gamma. \tag{16}$$

Remark 3.7. Based on the fact that the functions in $X_{h,C}$ are continuous across the edges on Γ and vanish on $\partial\Omega$, it is noted that

$$\langle A_{h,C} v, w\rangle = \sum_{j=1}^{J} a_j(v|_{\Omega_j}, w|_{\Omega_j}) \qquad \forall\, v, w \in X_{h,C}. \tag{17}$$

Here the bilinear form $a_j(\cdot,\cdot)$ is local to the subdomain Ω_j, which is defined as follows: for $v_j = v|_{\Omega_j}$ and $w_j = w|_{\Omega_j}$,

$$\begin{aligned} a_j(v_j, w_j) = &\sum_{\substack{T\in\mathcal{T}_h\\ T\subset\Omega_j}} \int_T \rho_j \nabla v_j \cdot \nabla w_j\, dx + \eta \sum_{\substack{e\in\mathcal{E}_h\\ e\subset\Omega_j}} \frac{\rho_j}{|e|} \int_e [\![v_j]\!] \cdot [\![w_j]\!]\, ds \\ &- \sum_{\substack{e\in\mathcal{E}_h\\ e\subset\Omega_j}} \int_e \Big(\{\!\{\rho_j \nabla v_j\}\!\} \cdot [\![w_j]\!] + \{\!\{\rho_j \nabla w_j\}\!\} \cdot [\![v_j]\!] \Big)\, ds. \end{aligned} \tag{18}$$

Based on the FETI-DP methodology, while paying attention to (17), we construct the operator $L_h : \hat{X}'_h \longrightarrow \hat{X}_h$ defined by

$$L_h(\hat{g}) = \hat{w} \qquad \forall\, \hat{g} \in \hat{X}'_h, \tag{19}$$

where $\hat{w}$ is characterized by the solution of the following problem:

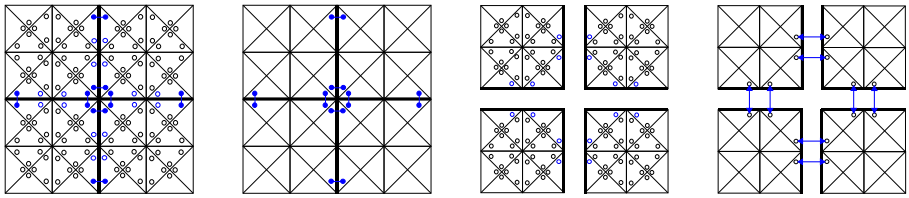

(a) (b) (c) (d)

FIGURE 3. (a) Degrees of freedom of $\hat{X}_h$. (b) Degrees of freedom related to the coarse problem. (c) Degrees of freedom related to the localized subdomain problems. (d) Pairs of neighboring vertices on Γ related to the introduced Lagrange multipliers.

Find $(\hat{w}, \lambda) \in \hat{X}_h \times \mathbb{R}^M$ such that

$$\sum_{j=1}^{J} a_j(\hat{w}|_{\Omega_j}, v|_{\Omega_j}) + \langle B^T\lambda, v\rangle = \int_\Omega \hat{g} v \, dx \qquad \forall\, v \in \hat{X}_h \tag{20}$$

$$\langle \mu, B\hat{w}\rangle = 0 \qquad \forall\, \mu \in \mathbb{R}^M, \tag{21}$$

where $\mathbb{R}^M$ is the space of Lagrange multipliers introduced on Γ and $\langle\cdot,\cdot\rangle$ is the Euclidean inner product in $\mathbb{R}^M$. Here, M represents the number of constraints used for imposing the pointwise matching on Γ, and B is a block matrix constructed from $\{0, 1, -1\}$ such that for any v in $\hat{X}_h$, $Bv = 0$ enforces v to be continuous across Γ; cf. Figure 3(d).

For the relacement of $A_{h,C}^{-1} : X_{h,C}^{'} \longrightarrow X_{h,C}$, we now define the operator $Q_h : X_{h,C}^{'} \longrightarrow X_{h,C}$ as follows:

$$Q_h = P_\Gamma L_h P_\Gamma^t, \tag{22}$$

where Q_h is represented in the following matrix form

$$\boldsymbol{Q} = \boldsymbol{P}_\Gamma \boldsymbol{L} \boldsymbol{P}_\Gamma^t. \tag{23}$$

Finally, we construct the preconditioner $\boldsymbol{P}_2$ for $\boldsymbol{A}$ by replacing $\boldsymbol{A}_C^{-1}$ with $\boldsymbol{Q}$:

$$\boldsymbol{P}_2 = \boldsymbol{I}_D \boldsymbol{A}_D^{-1} \boldsymbol{I}_D^t + \boldsymbol{I}_C \boldsymbol{Q} \boldsymbol{I}_C^t. \tag{24}$$

REMARK 3.8. The solver $\boldsymbol{L}$, resulting from the FETI-DP formulation in (20) and (21), consists of two main problems associated with the degrees of freedom depicted in Figure 3. One is the coarse solver related to the degrees of freedom at corner vertices; cf. Figure 3(b). The other is the subdomain solver related to the degrees of freedom localized to each subdomain; cf. Figure 3(c). Hence, the preconditioner $\boldsymbol{Q}$ involving $\boldsymbol{L}$ can be implemented efficiently by taking advantages of the structural properties of $\boldsymbol{L}$ described.

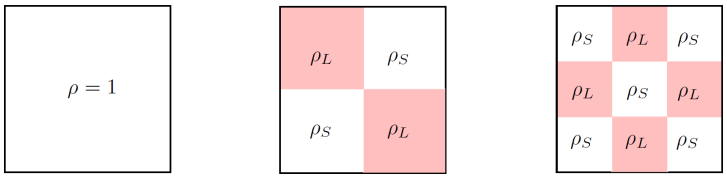

FIGURE 4. Left figure: Type A; Center figure: Type B; Right figure: Type C.

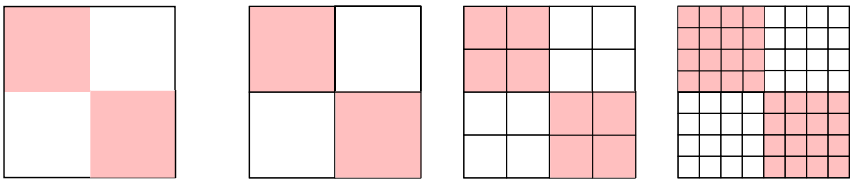

(a) (b)

FIGURE 5. (a) Piecewise constant coefficients ρ in a checkerboard pattern. (b) Decompositions of Ω into J subdomains for $J = 2 \times 2, 4 \times 4$, and 8×8.

4. Numerical results

In this section numerical results are presented, which show the performance of the proposed iterative method in terms of various parameters associated with the heterogeneous elliptic problem, the SIPG finite element discretization, and non-overlapping subdomain decomposition.

We consider a model problem (1) on the unit square $\Omega = (0,1) \times (0,1)$. Three different types of distributions of the coefficient ρ are tested throughout numerical experiments as described in Figure 4. The checkerboard pattern of ρ is characterized by two different constants ρ_S and ρ_L for $\rho_S \leq \rho_L$; cf. Type B and Type C in Figure 4

The discrete problem resulting the SIPG method is solved by the preconditioned conjugate gradient (CG) algorithm. For comparison, the CG iteration for solving (5) is also carried without preconditioning. The iteration is stopped when the relative residual is less than 10^{-6}. In Table 4 and Table 5, the sign $-$ in the CG Iter column indicates that the CG iteration fails to stop before the maximum number of iterations is reached, where the maximum number of iterations is set as the total number of unknowns of the discrete problem.

Here, discretization parameters h, H, and J are used, which stand for the mesh size, the subdomain size, and the number of subdomains, respectively. The domain Ω is divided into non-overlapping subdomains so that ρ is a constant on each subdomain. Throughout numerical tests, Ω is decomposed into J square subdomains with $J = 1/H \times 1/H$ where H denotes the length of the horizontal/vertical edges of the squares; cf. Figure 5(b). We use a uniform triangulation $\mathcal{T}_h$ of Ω; cf. Figure 2(a).

REMARK 4.9. For the stiffness matrix $\boldsymbol{A}$ and the matrices introduced in Section 4 for constructing the preconditioner $\boldsymbol{P}_2$, we denote the numbers of the degrees of freedom related to those matrices as follows:

$$\mathrm{Dof}(\boldsymbol{A}), \quad \mathrm{Dof}(\boldsymbol{A}_{\mathrm{D}}), \quad \mathrm{Dof}(\boldsymbol{A}_{\mathrm{C}}), \quad \mathrm{Dof}(\boldsymbol{L}).$$

For the decomposition into J subdomains with a uniform triangulation $\mathcal{T}_h$ of Ω depicted in Figure 2, Figure 3 and Figure 5(b), we have that

$$\begin{aligned}
\mathrm{Dof}(\boldsymbol{A}) &= \dim(X_h) = 12\left(\frac{1}{h}\right)^2, \\
\mathrm{Dof}(\boldsymbol{A}_D) &= \dim(X_{h,D}) = \frac{4}{h}\left(\frac{1}{H}+1\right), \\
\mathrm{Dof}(\boldsymbol{A}_C) &= \dim(X_{h,C}) = \frac{4}{h}\left(\frac{3}{h}-\left(\frac{1}{H}+1\right)\right), \\
\mathrm{Dof}(\boldsymbol{L}) &= \dim(\hat{X}_h) = \mathrm{Dof}(\boldsymbol{A}_C) + M = \mathrm{Dof}(\boldsymbol{A}_C) + 2\left(\frac{H}{h}-1\right)\left(\frac{1}{H}-1\right)\frac{1}{H},
\end{aligned}$$

where M is the number of Lagrange multipliers introduced for continuity constraints on Γ.

Remark 4.10. It is noted that $\boldsymbol{A}_D$ is a block diagonal matrix with small blocks. For example, in the case of $\frac{H}{h} > 2$, the blocks corresponding to the edges that do not touch any corners of subdomains are all 2×2; cf. Figure 2(c). Let $\mathcal{N}_C$ be the number of corners of subdomains. Hence the system involving $\boldsymbol{A}_D$ can be reduced to a system with $O(\mathcal{N}_C)$ degrees of freedom by solving a block diagonal system where each block is 2×2 and $\mathcal{N}_C = O\left(\left(\frac{1}{H}+1\right)^2\right)$.

Remark 4.11. Let us look into the problem formulated in (20) and (21). Once the dual solution λ is provided, the primal solution $\hat{w}$ can be found by solving the coarse problem and the subdomain problems; cf. Remark 3.8. Hence the system involving $\boldsymbol{L}$ can be reduced to a system $\boldsymbol{\Lambda}$ for the Lagrange multipliers, where $\mathrm{Dof}(\boldsymbol{\Lambda}) = M$. We pay attention not only to $\mathrm{Dof}(\boldsymbol{L})$ but also to $\mathrm{Dof}(\boldsymbol{\Lambda})$ since the matrix $\boldsymbol{L}$ does not need to be formed explicitly for PCG iterations.

Numerical results for the Type A pattern are presented in Table 2, which show the performance of $\boldsymbol{P}_2$ in terms of the number of iterations and the condition number. In developing iterative methods based on a DD approach, it is important to have the weak scalability and the strong scalability. First, the weak scalability of $\boldsymbol{P}_2$ is observed in Table 2 as the mesh size h decreases where the number of unknowns in the subdomains is fixed. Next, the strong scalability of $\boldsymbol{P}_2$ is also confirmed as the number of subdomains increases where the number of unknowns in the discrete problem is fixed.

Table 3 demonstrates that the performance of the preconditioner $\boldsymbol{P}_2$ is independent of the choice of η. For comparison, Table 3 also shows how the convergence rate deteriorates in the CG iterations without preconditioning as η increases.

The robustness of the preconditioner $\boldsymbol{P}_2$ with respect to the jump in ρ is demonstrated in Table 4, where $\rho_S = 1$ and ρ_L ranges between 1 and 10^5; cf. Figure 4 and Figure 5(b). In addition, the ill-conditioned property of $\boldsymbol{A}$ due to the increasing jump in ρ is observed, which agrees with the analysis presented in (6).

Based on the results confirmed in Table 2 to Table 4, numerical experiments are conducted for the Type B pattern, where $\frac{\rho_{\max}}{\rho_{\min}} = 10^5$. Results are presented in Table 5, which demonstrate that the performance of the preconditioner $\boldsymbol{P}_2$ for heterogeneous problems is similar to that of $\boldsymbol{P}_2$ for the problem of the Type A pattern.

Table 6 shows how the performance of the preconditioner $\boldsymbol{P}_2$ is affected by a variation of the jump ρ in the Type C pattern described in Figure 4, where $\rho_S = 1$ and $\rho_L = 10^5$. For comparison, the condition numbers are also presented for the Type A pattern.

TABLE 2. Performance of the preconditioner $\boldsymbol{P}_2$ in case of $\rho = 1$ where $\eta = 5$.

J	h	H/h	Dof($\boldsymbol{A}$)	$\boldsymbol{P}_2\boldsymbol{A}$				$\boldsymbol{A}$
				PCG Iter	κ	$\lambda_{\min}(\boldsymbol{P}_2\boldsymbol{A})$	$\lambda_{\max}(\boldsymbol{P}_2\boldsymbol{A})$	CG Iter
2×2	1/6	3	432	16	6.4544	3.0093e-1	1.9423	44
	1/12	6	1728	17	6.9447	2.7478e-1	1.9083	79
	1/24	12	6912	17	7.1341	2.6738e-1	1.9075	149
4×4	1/12	3	1728	17	6.5155	3.0111e-1	1.9618	79
	1/24	6	6912	18	6.9695	2.7368e-1	1.9074	149
8×8	1/24	3	6912	22	6.5336	2.9939e-1	1.9561	149

TABLE 3. Dependence of the preconditioner $\boldsymbol{P}_2$ on η where $\rho = 1$, $J = 4\times 4$, $h = 1/16$, and Dof($\boldsymbol{A}$) = 3072.

η	$\boldsymbol{P}_2\boldsymbol{A}$		$\boldsymbol{A}$	
	κ	PCG Iter	κ	CG Iter
5	6.7131	17	7.7883e+2	102
10	6.6701	17	1.5611e+3	137
50	1.2526e+1	23	7.7914e+3	253
100	1.4032e+1	24	1.5578e+4	299

TABLE 4. Robustness of the preconditioner $\boldsymbol{P}_2$ with respect to the jump in the coefficient ρ where $\rho_S = 1$, $\eta = 5$, $J = 4\times 4$, $h = 1/12$, and Dof($\boldsymbol{A}$) = 1728.

ρ_L	$\boldsymbol{P}_2\boldsymbol{A}$		$\boldsymbol{A}$	
	κ	PCG Iter	κ	CG Iter
1	6.5155	17	4.2383e+2	79
10^1	6.6161	17	1.3226e+3	200
10^2	6.7183	18	1.1169e+4	482
10^3	6.7301	18	1.1042e+5	–
10^4	6.7313	18	1.1030e+6	–
10^5	6.7314	18	1.1029e+7	–

TABLE 5. Performance of the preconditioner $\boldsymbol{P}_2$ in case of discontinuous coefficients ρ where $\rho_S = 1$, $\rho_L = 10^5$, and $\eta = 5$.

J	h	H/h	Dof($\boldsymbol{A}$)	$\boldsymbol{P}_2\boldsymbol{A}$				$\boldsymbol{A}$
				PCG Iter	κ	$\lambda_{\min}(\boldsymbol{P}_2\boldsymbol{A})$	$\lambda_{\max}(\boldsymbol{P}_2\boldsymbol{A})$	CG Iter
2×2	1/6	3	432	17	6.2808	3.0793e-1	1.9341	–
	1/12	6	1728	17	7.0052	2.7453e-1	1.9232	–
	1/24	12	6912	17	7.1852	2.6759e-1	1.9227	–
4×4	1/12	3	1728	18	6.7314	3.0056e-1	2.0232	–
	1/24	6	6912	19	7.3233	2.7355e-1	2.0033	–
8×8	1/24	3	6912	18	6.8009	2.9939e-1	2.0361	–

TABLE 6. Performance of the preconditioner $\boldsymbol{P}_2$ for two different types of coefficient distribution where $\eta = 5$ and $J = 3 \times 3$.

h	Type	$\kappa(\boldsymbol{P}_2\boldsymbol{A})$	$\kappa(\boldsymbol{A})$
1/18	A	6.9601	9.8213e+2
	C	6.9921	1.1314e+7
1/36	A	7.1389	3.9386e+3
	C	7.1872	4.4106e+7

5. Concluding remarks

In this paper we proposed an iterative method for the SIPG method, which is one of the best known DG methods. The proposed method has the unique feature that (i) an intermediate preconditioner is introduced by using the properties of discontinuous finite element functions and (ii) a preconditioning algorithm is constructed based on the FETI-DP methodology. Numerical studies on the proposed iterative method were presented, which showed that the preconditioner performs well in terms of various parameters such as the diffusion coefficient, the penalty parameter, the mesh size, the subdomain size, and the number of subdomains.

Meanwhile, the iterative method developed in this paper can be extended to other types of DG method treated in [2] and the case of non-conforming meshes; cf. [5]. In addition, the extension to the three-dimensional problem can be designed based on the modification of the subspace decomposition and the introduction of a larger coarse problem than that used for the problem in 2D; cf. [18,23]. Including these extensions, further studies on theoretical performance analysis will be conducted elsewhere.

Acknowledgments. The author would like to sincerely thank Professor Susanne C. Brenner and Professor Li-yeng Sung for taking the time to have a valuable discussion.

References

[1] P. F. Antonietti and B. Ayuso, *Schwarz domain decomposition preconditioners for discontinuous Galerkin approximations of elliptic problems: non-overlapping case*, ESIAM:M2AN. **41** (2007), 21–54.

[2] D. Arnold, F. Brezzi, B. Cockburn, and L. Marini, *Unified analysis of discontinuous Galerkin methods for elliptic problems*, SIAM J. Numer. Anal. **39** (2002), 1749–1779.

[3] D. N. Arnold, *An interior penalty finite element method with discontinuous elements*, SIAM J. Numer. Anal. **19** (1982), 742–760.

[4] S. Brenner, E.-H. Park, and L.-Y. Sung, *A BDDC preconditioner for a weakly over-penalized symmetric interior penalty method*, Numer. Linear Alg. Appl. **20** (2013), 472–491.

[5] S. C. Brenner, E.-H. Park, and L.-Y. Sung, *A BDDC preconditioners for a symmetric interior penalty Galerkin method*, Electron. Trans. Numer. Anal. **46** (2017), 190–214.

[6] S. C. Brenner and L. R. Scott, *The Mathematical Theory of Finite Element Methods (Third Edition)*, Springer-Verlag, New York, 2008.

[7] S. C. Brenner and L.-Y. Sung, *BDDC and FETI-DP without matrices or vectors*, Comput. Methods Appl. Mech. Engrg. **196** (2007), 1429–1435.

[8] C. Canuto, L. F. Pavarino, and A. B. Pieri, *BDDC preconditioners for continuous and discontinuous Galerkin methods using spectral/hp elements with variable local polynomial degree*, IMA J. Numer. Anal. **34** (2014), 879–903.

[9] L. T. Diosady and D. L. Darmofal, *A unified analysis of balancing domain decomposition by constraints for discontinuous Galerkin discretizations*, SIAM J. Numer. Anal. **50** (2012), 1695–1712.

[10] M. Dryja, *On discontinuous Galerkin methods for elliptic problems with discontinuous coefficients*, Comput. Methods Appl. Math. **3** (2003), 76–85.

[11] M. Dryja, J. Galvis, and M. Sarkis, *BDDC methods for discontinuous Galerkin discretization of elliptic problems*, J. of Complexity **23** (2007), 715–739.

[12] M. Dryja, J. Galvis, and M. Sarkis, *The analysis of a FETI-DP preconditioner for a full DG discretization of elliptic problems in two dimensions*, Numer. Math. **131** (2015), 737–770.

[13] C. Farhat, M. Lesoinne, P. Le Tallec, and K. Pierson, *FETI-DP: A dual-primal unified FETI method - part I: A faster alternative to the two-level FETI method*, Int. J. Numer. Methods Engrg. **50** (2001), 1523–154.

[14] C. Farhat, M. Lesoinne, and K. Pierson, *A scalable dual-primal domain decomposition method*, Numer. Lin. Alg. Appl. **7** (2000), 687–714.

[15] X. Feng and O. A. Karakashian, *Two-level non-overlapping Schwarz preconditioners for a discontinuous Galerkin approximation of the biharmonic equation*, J. Sci. Comput. **22** (2005), 289–314.

[16] D. Z. Kalchev and P. Vassilevski, *Auxiliary space preconditioning of finite element equations using a nonconforming interior penalty reformulation and static condensation*, SIAM J. Sci. Comput. **42** (2020), 1741–1764.

[17] H. H. Kim, E. T. Chung, and C. S. Lee, *FETI-DP preconditioners for a staggered discontinuous Galerkin formulation of the two-dimensional Stokes problem*, Comput. Math. Appl. **68** (2014), 2233–2250.

[18] A. Klawonn, O. B. Widlund, and M. Dryja, *Dual-Primal FETI methods for three dimensional elliptic problems with heterogeneous coefficients*, SIAM J. Numer. Anal. **40** (2002), 159–176.

[19] J. Li and O. B. Widlund, *FETI-DP, BDDC, and block Cholesky methods*, Internat. J. Numer. Methods Engrg. **66** (2006), 250–271.

[20] J. Mandel and C. R. Dohrmann, *Convergence of a balancing domain decomposition by constraints and energy minimization*, Numer. Linear Algebra Appl. **10** (2003), 639–659.

[21] J. Mandel and R. Tezaur, *On the convergence of a dual-primal substructuring method*, Numer. Math. **88** (2001), 543–558.

[22] J. Douglas, Jr. and T. Dupont, *Interior penalty procedures for elliptic and parabolic Galerkin methods*, Computing methods in applied sciences, Lecture Notes in Phys., 58, Springer, Berlin, 1976.

[23] B. Rivière, *Discontinuous Galerkin Methods for Solving Elliptic and Parabolic Equations - Theory and Implementation*, SIAM, Philadelphia, 2008.

[24] A. Toselli and O. B. Widlund, *Domain Decomposition Methods - Algorithms and Theory*, Springer-Verlag, Berlin, 2005.
[25] M. F. Wheeler, *An elliptic collocation-finite element method with interior penalties*, SIAM J. Numer. Anal. **15** (1978), 152–161.

Eun-Hee Park
Department of Artificial Intelligence and Software,
Kangwon National University, Samcheok 25913, Korea
E-mail: eh.park@kangwon.ac.kr